



must be used to match the component of wave vector of the incident light parallel to the surface to the SP wave vector.

For thin film structures of limited number of layers, the analytical calculation of the reflectance is straightforward. However, when the number of layers exceeds three, it becomes cumbersome to derive an analytical expression of the reflectance. Therefore, a standard matrix formalism (Azzam and Bashara 1979) can be utilized instead. To fit the matrix calculated reflectance to the measured attenuated total reflectance (ATR), we have chosen the Simplex minimization technique which appeared to be the most suitable because the theoretical model is non-linear.

The aim of this paper is to show that SPs excitations can be used to extract optical and geometrical parameters of specific layers in multi-layered thin film systems. This can be achieved by fitting the measured ATR to the calculated reflectance using the Simplex method (Nelder and Mead 1965). The plan of this paper is as follows. In the first section, the experimental technique for measuring ATR is described and the standard matrix formalism is briefly presented. Previously obtained experimental reflectance data by one of us (Tamm *et al* 1993), for an Al/GaAs sample, is used to probe the optical properties and thickness of the Al-oxide layer. The second section is devoted to results and discussion, and we show how sensitive is the theoretical reflectance to certain parameters. Concluding remarks are made in the last section.

### Experiment and Theory of Reflectance

The experimental data (reflectance versus angle of incidence) were taken using an Otto configuration Prism / air gap / Al-oxide / Al / GaAs shown in Figure.1 (Otto 1969). The sample (Al/GaAs) is separated from the prism by an air gap of the wavelength order. The Al-oxide and Al thickness nominal values are 4 nm and 22 nm respectively.

For angle of incidence in the prism,  $\theta_i$  greater than the critical angle  $\theta_c$ , incident light of wave-vector  $k_i$  couples via the evanescent field in the air-gap to the SPs (wave-vector  $k_{SP}$ ) to the metal surface with conservation of the component of the wave-vector parallel to the interfaces  $k_{SP} = k_i n \sin \theta_i$ , with  $n$  being the refractive index of the prism. The air-gap here acts as an optical tunneling barrier from which extends the evanescent optical field to the Al / air interface. Varying  $\theta_i$ , allows the tuning of the incident light wave vector to that of SPs until they are matched creating the resonance condition.

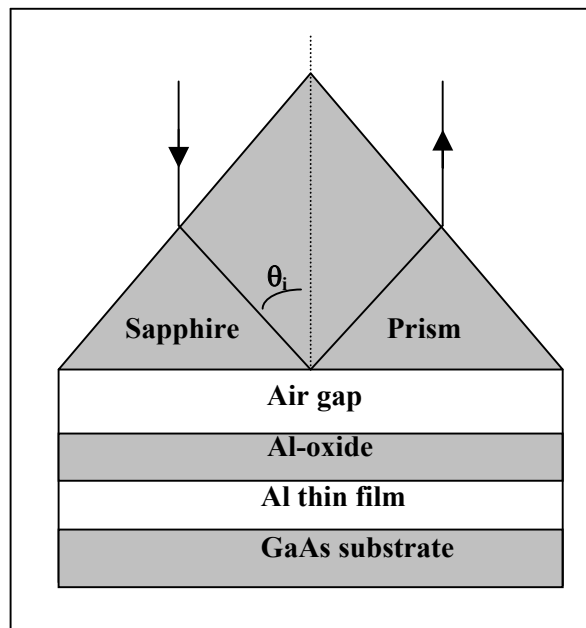


**Figure 1.** Detail of arrangement for making Otto configuration ATR measurements on Al / GaAs sample.

The prism-sample configuration is rotated under computer control with the reflected beam and reference beam recorded at 1000 points across any given angle scan range. The incident p-polarized

## SURFACE PLASMONS FOR PROBING OPTICAL DATA OF MULTI-LAYERED THIN FILMS

beam of a given wavelength is produced by passing randomly polarized radiation from a light source through a CaF<sub>2</sub> based polarizer. The incident radiation is mechanically chopped at 1 kHz and standard phase sensitive detection techniques are employed to monitor the reflected and reference beams that impinge on a suitable detector. The p-polarized reflected signal divided by the reference signal is scaled to give attenuated total reflectance (ATR) as a function of internal angle of incidence.

The interpretation and modeling of the measured ATR requires the theoretically calculated reflectance. Standard electromagnetic theory of light is routinely used to derive expressions for the complex amplitude reflection coefficients in terms of the microscopic optical properties and thickness of the different constituent layers of a given structure. The propagation of plane waves in an isotropic medium is described by the complex index of refraction  $N = n - j k$ ,  $n$  is the real index of refraction and  $k$  is the extinction coefficient. The reflection and transmission are calculated using a 2 x 2 matrix formalism described in details in Azzam and Bashara (1979). Following this formalism, if  $E^+(z)$  and  $E^-(z)$  are the complex amplitudes of the forward and backward travelling waves perpendicular to the interface between two layers, the total field is denoted by:

$$E(z) = \begin{bmatrix} E^+(z) \\ E^-(z) \end{bmatrix}$$

Assuming that the equations describing the propagation of light are linear and that the tangential fields across any interface between two adjacent layers are continuous, the fields  $E^+(z')$  and  $E^-(z'')$  at two different planes  $z'$  and  $z''$  are related by a 2 x 2 matrix transformation:

$$\begin{bmatrix} E^+(z') \\ E^-(z'') \end{bmatrix} = \begin{bmatrix} S_{11} & S_{12} \\ S_{21} & S_{22} \end{bmatrix} \cdot \begin{bmatrix} E^+(z'') \\ E^-(z'') \end{bmatrix} \quad \text{or} \quad E(z') = S E(z'') \quad (1)$$

$S$  is a scattering matrix characteristic of the part of the structure confined between the planes  $z'$  and  $z''$ . For a structure of  $m$  layers and  $m-1$  interfaces confined between ambient (0) and substrate ( $m+1$ ),  $S$  can be written as  $S = \sum_{i=1}^{m+1} I_{(i-1)i} L_i$  where  $I_{(i-1)i}$  is a 2 x 2 matrix characteristic of the interface ( $i-1$ )I and  $L_i$  is a 2 x 2 matrix characteristic of the  $i^{\text{th}}$  layer. In fact, if  $z'$  and  $z''$  are on opposite sides of the interface between layers ( $i-1$ ) and  $i$ , equation (1) becomes:

$$E(z_i - 0) = I_{(i-1)i} E(z_i + 0)$$

However, if  $z'$  and  $z''$  are both inside the  $i^{\text{th}}$  layer, equation (1) becomes:

$$E(z_i + 0) = L_i E(z_i + d_i - 0) \quad \text{with } d_i \text{ the thickness of the layer.}$$

With no reflected wave in the substrate, the fields in the ambient (a) and substrate (s) are related by

$$\begin{bmatrix} E_a^+ \\ E_a^- \end{bmatrix} = S \begin{bmatrix} E_s^+ \\ 0 \end{bmatrix}.$$

For a given layer  $i$  and interface  $i-1$ , the matrices  $I_{(i-1)i}$  and  $L_i$  can be written as

$$I_{(i-1)i} = \frac{1}{t_{(i-1)i}} \begin{bmatrix} 1 & r_{(i-1)i} \\ r_{(i-1)i} & 1 \end{bmatrix} \quad ; \quad L_i = \begin{bmatrix} e^{j\beta} & 0 \\ 0 & e^{j\beta} \end{bmatrix},$$

where  $t_{(i-1)i}$  and  $r_{(i-1)i}$  are the Fresnel reflection coefficients of the (i-1)i interface and  $\beta$  is the layer phase thickness and it is given by  $\beta = \frac{2\pi dN}{\lambda} \cos \phi$  with  $\phi$  representing the angle between the direction of propagation in the  $i^{\text{th}}$  layer and the normal to the interface. Subsequent to calculating the different layer and interface matrices for a given stratified structure, the overall reflection can be determined from:

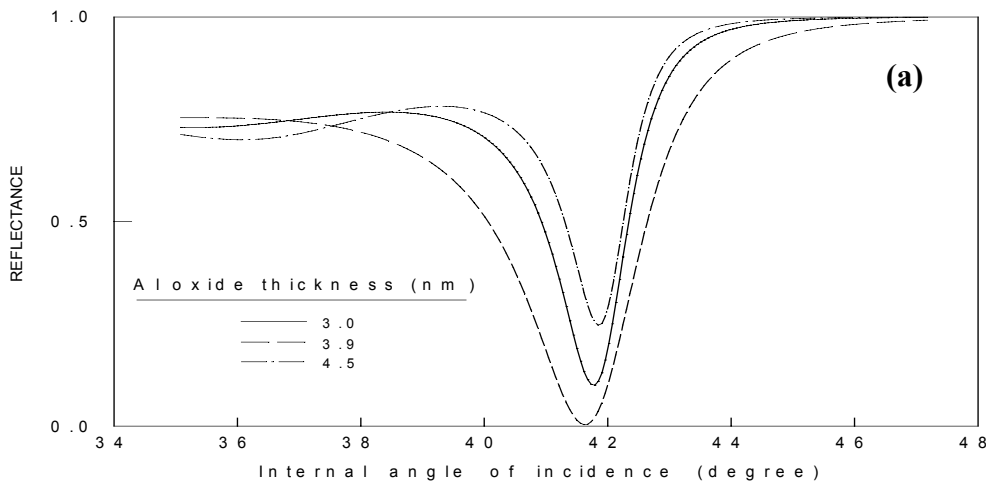
$$R = \frac{E_a^-}{E_a^+} = \frac{S_{21}}{S_{11}}$$

A Fortran program was implemented to evaluate the different matrices, obtain  $S_{11}$  and  $S_{21}$  for p-polarized light and yield the reflectance R. These calculations were carried out at various angles of incidence  $\theta_i$  and for different optical and geometrical parameters of the Otto configuration described above.

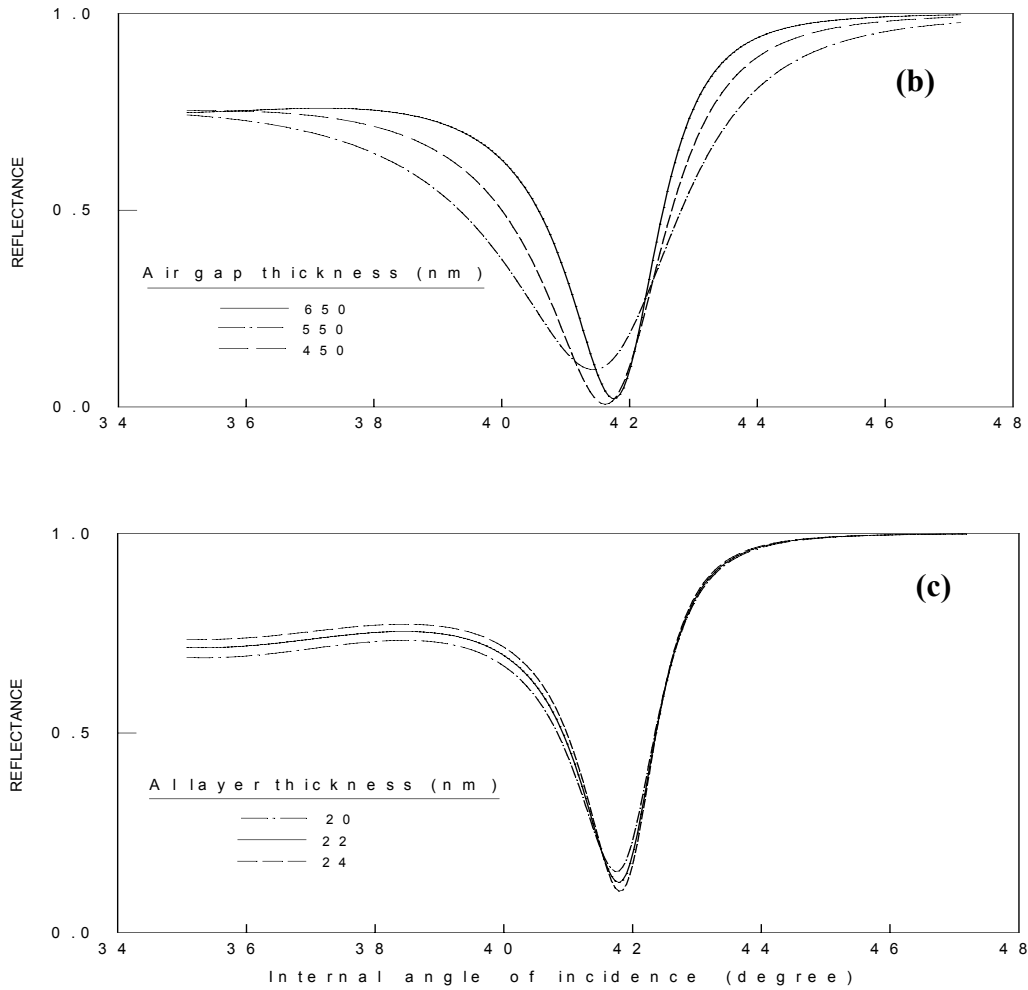
### Results and Discussion

Figure 2 (a) and (b) show the calculated reflectance using the matrix formalism for different thicknesses of Al-oxide layer and air gap respectively. For both graphs, increasing slightly the thickness results in increasing the reflectance minimum as well as shifting the resonance angle. Note that the air gap value is kept around the incident light wavelength magnitude and the Al-oxide thickness is around the nominal value. As discussed extensively by Tamm *et al* 1991, the depth of the SP's reflectance minimum is primarily determined by the dimension of the air coupling gap. This theoretical model assumes no wedging in the air gap which is plausible for a small diameter laser beam tracking across the prism-air gap interface as the prism-sample assembly is rotated.

The effect of the Al thin film thickness around the nominal value (22 nm) on the calculated reflectance is shown in Figure 2(c). Here, we notice almost no change of the resonance curve at high angles and a minor shift of the resonance angle. However, a significant change appears at lower angles.



## SURFACE PLASMONS FOR PROBING OPTICAL DATA OF MULTI-LAYERED THIN FILMS



**Figure 2.** The calculated reflectance as a function of incidence angle for different:  
 (a) Al-oxide thickness, Al and air gap thickness are 22 nm and 650 nm respectively.  
 (b) Air gap thickness, Al-oxide and Al thickness are 3.4 nm and 22 nm respectively.  
 (c) Al thickness, Al-oxide and air gap thickness are 3.4 and 650 nm respectively. For the three graphs, the wavelength is 633 nm and the Al-oxide optical constant is 3.

The effect of the Al thin film thickness around the nominal value (22 nm) on the calculated reflectance is shown in Figure 2(c). Here, we notice almost no change of the resonance curve at high angles and a minor shift of the resonance angle. However, a significant change appears at lower angles.

The calculated reflectance for different Al-oxide optical constant at constant incident light wavelength (633 nm) is shown in Figure 3. It is interesting to note that the curve shifts in the region around the resonance angle only. The literature values of  $\text{Al}_2\text{O}_3$  optical data (table1) show a minor dispersion for different wavelengths and therefore varying Al-oxide optical constant around the reported value implies considering an oxide layer of different optical nature.

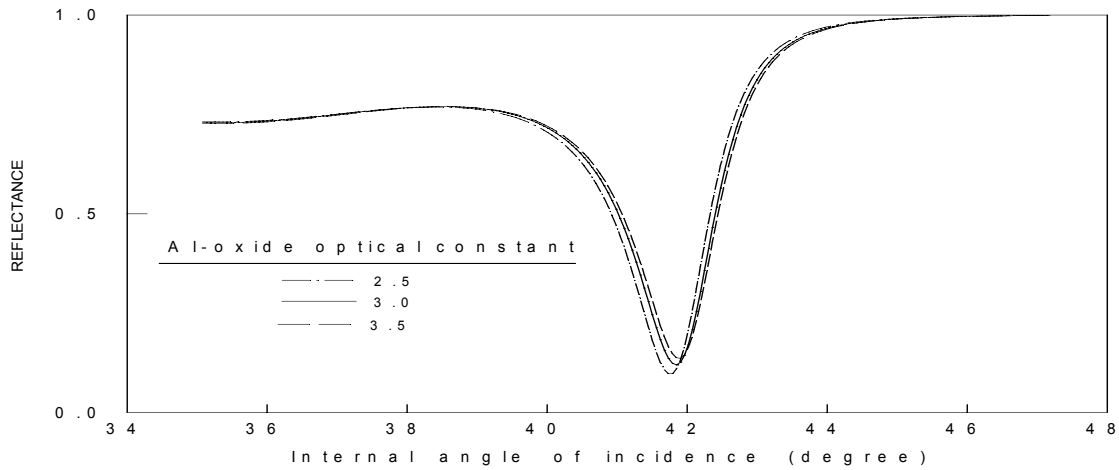


**Figure 3.** The calculated reflectance as a function of incidence angle for different Al-oxide optical constant. The wavelength is 633 nm. The air gap, Al-oxide and Al thickness are 650 nm, 3.4 nm and 22 nm respectively.

**Table 1:** Fitting parameters of measured ATR to calculated reflectance for the multi-layered system prism/air gap/Al oxide/Al/GaAs at different incident light wavelengths obtained to produce the theoretical curves of Figure 5. The invariant parameters of the modeled reflectance were taken from the literature.  $\epsilon_r$  and  $\epsilon_i$  are the real and imaginary parts of the dielectric function and  $t$  is the thickness of each medium of the multi-layered system.

Fitting parameters				Invariant parameters						
$\lambda$ (nm)	Air gap	Al-oxide		Al	Prism (Ref.1)	Al (Ref.1)		GaAs (Ref.2)		Al-oxide (Ref.1)
	t(nm)	$\epsilon_r$	t(nm)	t(nm)	$\epsilon_r$	$\epsilon_r$	$\epsilon_i$	$\epsilon_r$	$\epsilon_i$	$\epsilon_r$
633	772	2.98	3.50	24.4	2.298	-37.3	13.7	14.8	1.5	3.0
590	593	2.72	4.19	24.5	2.300	-33.0	11.3	15.5	1.9	3.1
458	506	3.31	3.90	23.1	2.324	-21.1	4.7	20.5	5.4	3.13

Ref.1: Tamm *et al* 1993; Ref.2: Palik 1985.

Concurrently, the same equations developed for reflectance calculations are readily utilized to obtain the evanescent field (E-field), for a particular incident angle  $\theta_i$  and wavelength  $\lambda$ , in each of the structure layers. The examination of the field profile, shown in Figure 4, and calculated for the geometry Prism / Air gap / Al / GaAs at resonance  $\theta_i = 41.8^\circ$  and  $\lambda = 633$  nm reveals the surface nature of the mode excited here. The field is evanescent in the air gap, decaying away from the Al / air interface into both air and Al with respective decaying lengths of approximately 600 nm and 10 nm. The field is however, oscillatory in both the incident medium (prism) and the GaAs substrate, indicating the radiating nature of the EM fields in these media.

## SURFACE PLASMONS FOR PROBING OPTICAL DATA OF MULTI-LAYERED THIN FILMS

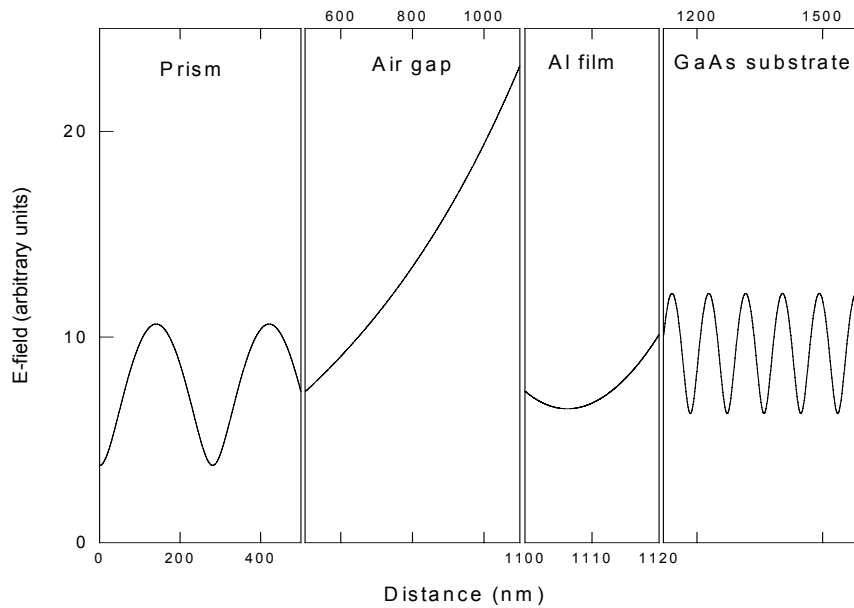


**Figure 4.** The calculated E-field as a function of distance in each medium of the geometry Prism / Air gap / Al / GaAs, at resonance angle  $\theta_i = 41.8^\circ$  and wavelength  $\lambda = 633$  nm.

The measured ATR on the multi-layered system Prism/Air gap/Al-oxide/Al/GaAs has been fitted to the matrix calculated reflectance by minimizing the sum of the squared residuals using the Simplex method. For this purpose, a Fortran code on a personal computer has been implemented. The four fitting parameters were those described above showing the reflectance sensitivity, namely: the Al-oxide optical constant, the thickness of the air gap, Al-oxide and Al.

In this process, the real and imaginary parts of the dielectric function for Al, GaAs and the glass prism were based on values given in the literature (Tamm *et al* 1993, Palik 1985); at given wavelength, these parameters were treated as invariant in the modeling process. Fits for different light wavelengths are shown in Figure 5. Fitting and invariant parameters are in table 1.

As can be seen, the 633 nm wavelength data shows a very good fit as well as good agreement of the modeled Al-oxide optical constant with the  $\text{Al}_2\text{O}_3$  literature value (table 1). Moreover, at this wavelength, the modeled thickness of the air gap, Al-oxide and Al are consistent with the nominal values.

On the other hand, the fits of 590 nm and 458 nm wavelengths are not as good in particular around the resonance region. As expected their corresponding Al-oxide optical constants are far from the known values. The interpretation of this discrepancy may be related primarily to the wedging effect of the air gap in addition to a less pronounced dispersion effect of the Al-oxide layer. We mentioned above that the theoretical model assumes no air gap wedging which is plausible as long as the light beam is small. Indeed, it is the case for the 633 nm wavelength produced by a laser source but not for 590 nm and 458 nm light beams produced by an ordinary collimated source. Furthermore, having different optical constants at different wavelengths for the Al-oxide layer might suggest the presence of other substances, above and/or under  $\text{Al}_2\text{O}_3$ , with dispersion effect on the incident light.

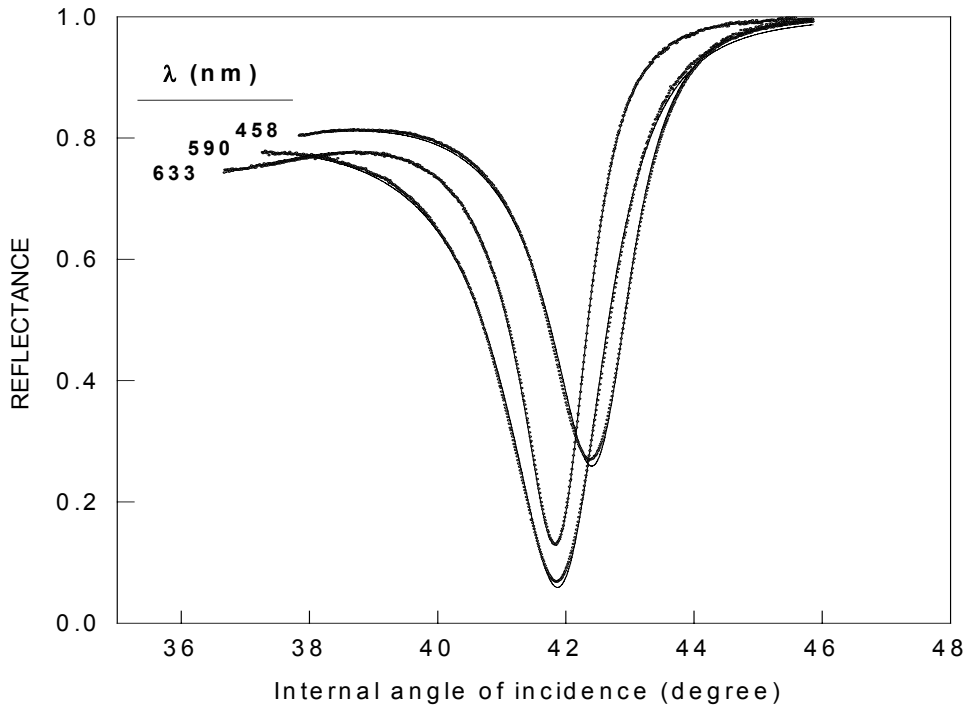


**Figure 5.** Fit of the measured ATR (dots) to the calculated reflectance (line) as a function of the internal angle of incidence for different wavelengths. Fitting and invariant parameters are shown in table 1.

For all three wavelengths, the modeled Al-oxide thickness is of the order of a few atomic layers. However it appears higher for wavelengths 590 nm and 458 nm than 633 nm. This might also suggest the presence of extra layers. The last point to be highlighted concerns the response of the structure to incoming light. The electron gas response of the Al metallic layer is determined strongly by the large imaginary part of the dielectric function at all wavelengths considered here. This means that the mode excited is that of SPs with the plasmon response being slightly weaker at shorter wavelength than the response at  $\lambda = 633$  nm; the value of the real part of the Al dielectric function  $\epsilon_r$  is smaller in absolute value (see table 1). Nevertheless,  $\epsilon_r$  remains very much less than  $-1$  and larger than the imaginary part  $\epsilon_i$ . This fulfils the well-known condition for existence of SPs and excludes the possibility of losing a dielectric surface mode which might be present otherwise (under for example the condition  $\epsilon_r > 0$  and  $|\epsilon_r| > \epsilon_i$ ).

### Conclusion

In this paper, we have shown how optical excitation of surface plasmons (SPs) can be used to obtain optical and geometrical parameters of specific layers in the multi-layered system: Prism / Air gap / Al-oxide / Al / GaAs. The modeled Al-oxide optical constant at 633 nm wavelength agrees well with the literature but show a dispersion effect at 590 nm and 458 nm wavelengths in disagreement with the reported values. The geometrical parameters such as the thickness of air gap, Al-oxide and Al are consistent with the nominal values.

Considering these results, we may propose this method for probing unknown optical and geometrical data of uncertain layers in any thin film systems where good and reliable data is available for the known constituent layers. The method may also be a good technique for monitoring the thickness of thin films growing.

# SURFACE PLASMONS FOR PROBING OPTICAL DATA OF MULTI-LAYERED THIN FILMS

## References

- AZZAM, R.M.A. and BASHARA, N.M. 1979. *Ellipsometry and Polarized Light*. North Holland. Amsterdam.
- NELDER, J.A. and MEAD, R. 1965. A Simplex Method for Function Minimization. *Comp.J.*, **7**: 308-313.
- OTTO, A. 1968. Excitation of Non-Radiative Surface Plasma waves in Silver by the Method of Frustrated Total Reflection. *Z. Physik*, **26**: 398-415.
- PALIK, E.D. (Editor). 1985. *Handbook of Optical Constants of Solids*, 429. Academic Press. London.
- RAETHER, H. 1988. *Surface Plasmons on Smooth and Rough Surfaces and on Gratings*. Springer-Verlag.
- TAMM, I.R., DAWSON, P., CONNOLLY, M.P., RAZA, S.H. and GAMBLE, H.S. 1991. Fast and Slow Mode Plasmons in Ag – Al. *J.Mod. Optics*, **38**: 1593- 1615.
- TAMM, I.R., DAWSON, P., SELLA, A., PATE, M.A., GREY, R. and HILL, G. 1993. Analysis of Surface Plasmon Polariton Enhancement in Photodetection by Schottky Diodes, *Sol.St.Electronics* **36**: 1417-1427.
- 

Received 20 December 1999

Accepted 18 August 2000